The Magnetic Structure of Hα Macrospicules in Solar Coronal Holes

Y. Yamauchi[1] R. L. Moore, S. T. Suess

NASA Marshall Space Flight Center, Mail Code SD50, Huntsville, AL 35812

Yohei.Yamauchi@msfc.nasa.gov, Ron.Moore@msfc.nasa.gov,
Steven.T.Suess@nasa.gov

H. Wang

Big Bear Solar Observatory, New Jersey Institute of Technology, Big Bear City, CA 92314

haimin@flare.njit.edu

and

T. Sakurai

National Astronomical Observatory of Japan, 2-21-1 Osawa, Mitaka, Tokyo 181-8588, Japan

sakurai@solar.mtk.nao.ac.jp

ABSTRACT

Measurements by Ulysses in the high-speed polar solar wind have shown the wind to carry some fine-scale structures in which the magnetic field reverses direction by having a switchback fold in it. The lateral span of these magnetic switchbacks, translated back to the Sun, is of the scale of the lanes and cells of the magnetic network in which the open magnetic field of the polar coronal hole and polar solar wind are rooted. This suggests that the magnetic switchbacks might be formed from network-scale magnetic loops that erupt into the corona and then undergo reconnection with the open field. This possibility motivated us to undertake the study reported here of the structure of Hα macrospicules observed at the limb in polar coronal holes, to determine whether a significant fraction of these eruptions appear to be erupting loops. From a search of the polar

[1]NRC/NAS Resident Research Associate

coronal holes in 6 days of image-processed full-disk Hα movies from Big Bear Solar Observatory, we found a total of 35 macrospicules. Nearly all of these (32) were of one or the other of two different forms: 15 were in the form of an erupting loop, and 17 were in the form of a single-column spiked jet. The erupting-loop macrospicules are appropriate for producing the magnetic switchbacks in the polar wind. The spiked-jet macrospicules show the appropriate structure and evolution to be driven by reconnection between network-scale closed field (a network bipole) and the open field rooted against the closed field. This evidence for reconnection in a large fraction of our macrospicules (1) suggests that many spicules may be generated by similar but smaller reconnection events, and (2) supports the view that coronal heating and solar wind acceleration in coronal holes and in quiet regions are driven by explosive reconnection events in the magnetic network.

Subject headings: Sun: chromosphere—Sun: magnetic fields—Sun: corona

1. Introduction

Solar coronal heating and solar wind acceleration are among the fundamental unsolved problems in solar physics. Many solar scientists expect that the magnetic field permeating the corona and solar wind is essential for much of the heating and acceleration. Many previous investigations have searched for clues to these processes in observations of the corona and solar wind. In this paper, we look for clues in the roots of the magnetic field, in the chromosphere, by examining the magnetic form and development of macrospicules observed in Hα at the limb in polar coronal holes.

Macrospicules are eruptive events that are generally of columnar form. They appear to be giant spicules or small surges (Beckers 1977; Tandberg-Hanssen 1977). They were discovered in *Skylab* He II 304 Å images as cool ($\sim 8 \times 10^4$ K) material extending into the corona above the limb in coronal holes (Bohlin et al. 1975). They reach heights of 7000 – 40,000 km above the limb, have rise velocities of 10 – 150 km s^{-1}, and have lifetimes of 3 – 45 minutes (Dere et al. 1989; Karovska & Habbal 1994). They are concentrated in the polar coronal holes. Macrospicules are visible at various wavelengths, such as Hα (e.g., Moore et al. 1977; LaBonte 1979; Loucif 1994; Karovska & Habbal 1994) and radio (Habbal & Gonzalez 1991) as well as EUV (e.g., Bohlin et al. 1975; Withbroe et al. 1976; Dere et al. 1989). However, Wang (1998) found that the morphology of a macrospicule in He II 304 Å is often very different from that seen in Hα in the same event, and that over 50% of the Hα macrospicules in the polar regions are not visible in He II 304 Å.

The formation mechanism of macrospicules is controversial. In particular, it is uncertain whether the eruptive mass motion is mainly driven directly by the magnetic field (by the $\boldsymbol{J} \times \boldsymbol{B}$ force) or indirectly by an explosive increase in gas pressure at the base from heating by a flare-like dissipation of magnetic energy (Shibata 2001). Moore et al. (1977) showed that some Hα macrospicules have an X-ray bright point flare at their base. From this, they suggested that all macrospicules and spicules may be produced by similar, but usually smaller, explosive releases of magnetic energy. This leaves open the question of whether the force that drives the ejection is mainly magnetic or mainly from gas pressure. In an attempt to explain the production of Hα macrospicules as well as EUV macrospicules not seen in Hα, Shibata (1982) used a jet model in which a gas pressure pulse at the base drives a shock wave up along open magnetic field lines. However, in this model it is difficult for the shock to be strong enough to lift the expelled material to the observed heights of macrospicules ($>\sim 10^4$ km) without making the gas too hot to be visible in Hα (Shibata 2001). An alternative model for X-ray jets and Hα surges uses the fact that these eruptions are observed to be rooted around an inclusion of opposite polarity magnetic flux (e.g., Shibata et al. 1992; Yokoyama & Shibata 1995, 1996; Shibata 2001). In this situation, there is a magnetic null between open and closed magnetic field lines. Reconnection at the null can both drive cool (Hα) plasma up along the open magnetic field (via the slingshot effect of the field released by the reconnection) and heat some plasma (via shocks and resistive dissipation) to EUV and X-ray temperatures. This reconnection model for X-ray jets and Hα surges is a promising candidate for macrospicules, provided that macrospicules have inclusions of opposite polarity magnetic flux at their base.

Photospheric magnetograms show that, while the magnetic flux in coronal holes is predominantly of one polarity, there is a fine-scale admixture of opposite-polarity flux scattered throughout the network, amounting to about 10% of the total flux (e.g., Lin 1994; Bumba, Klvaňa, & Sýkora 1994; DeForest et al. 1997). That is, the magnetic network in coronal holes, as in all quiet regions, is peppered with local inclusions of opposite polarity, and hence the network should be well populated with local magnetic loops (e.g., Dowdy, Rabin, & Moore 1986). Thus, the magnetic polarity arrangement in the network in coronal holes is favorable for production of macrospicules along the lines of the Shibata reconnection model.

From *Skylab* EUV spectroheliograms having spatial resolution of about 5″, Karovska & Habbal (1994) showed that there is arch-like structure at the base of some large macrospicules, and that in some cases the arch appears to balloon upward and burst open during the growth of the macrospicule. From 5″ resolution He II 304 Å images from SOHO/EIT and subarcsecond resolution Hα images from Big Bear Solar Observatory (BBSO), Wang (1998) found that, while usually only a lower part of a He II 304 Å macrospicule could be seen in Hα, the high resolution of the Hα images showed that the base of the macrospicule often had arch-

like or double-column structure. Furthermore, from subarcsecond resolution Hα images from BBSO, Tanaka (1972, 1974) found that about 30% of Hα dark mottles rooted in the network (i.e., spicules observed on the disk) show a double-strand structure. This suggests to us that these spicules might be formed by the eruption of a small network magnetic loop, the two strands being the legs of the erupted loop. Since macrospicules appear to be large versions of spicules, the high incidence of double-strand spicules along with the above observations of Karovska & Habbal (1994) and Wang (1998), suggests that many macrospicules might be formed by the eruption of larger network magnetic loops. The formation process for these macrospicules would be different from that in the Shibata reconnection model. In any case, all of the observations noted in this and the previous paragraph encourage the view that macrospicules and spicules are produced by localized explosive releases of magnetic energy in the network.

Separate from the above observations, there is another line of evidence that also suggests that magnetic loops in the network often erupt to great heights in coronal holes. The magnetic field in the solar wind from a polar coronal hole is expected to be directed all outward or all inward, so that it is in agreement with the polarity of the open magnetic field filling the coronal hole. Ulysses measurements in the high-speed solar wind at polar latitudes show that nearly all of the magnetic field does have the expected direction, but that the polar wind has in it some fine-scale structures in which the field is reversed (e.g., Forsyth et al. 1996; Balogh et al. 1999; Yamauchi et al. 2002). The duration of such magnetic reversal is typically a couple of 10 minutes to ≤ 2 hours, which corresponds to a heliographic lateral span $\leq 1^\circ$ ($= 10^4$ km) on the surface of the Sun. This is roughly the width of the magnetic lanes of the network (Falconer et al. 1998). Yamauchi et al. (2002) proposed that the magnetic reversals in the polar wind are produced by eruptive events in the magnetic network. From further analysis of the Ulysses observations, Yamauchi et al. (2003) have found that nearly all of the field reversals in the polar wind are switchback folds in the magnetic field. A fold of the observed scale could be produced by the eruption of a macrospicule-size magnetic loop from the magnetic network, followed by reconnection with the open magnetic field of the coronal hole, as depicted in Figure 1. If the loop-opening reconnection is not completed until the top of the loop enters the acceleration region of the wind, then the magnetic switchback could be caught in the outflow and persist in the polar wind. Thus, the observed fine-scale magnetic switchbacks in the polar wind motivated us to search for network-scale erupting magnetic loops in polar coronal holes.

In this paper, we report a systematic study of the magnetic morphology of Hα macrospicules observed on the limb in polar coronal holes. At the outset of the study our main goal was to determine whether a significant fraction of these macrospicules appear to be erupting magnetic loops. We find that a large minority (43%) does have this form, and hence that

erupting magnetic loops of the appropriate size to become the magnetic switchbacks are a common occurrence in polar coronal holes. In addition, we find that about half of the macrospicules are distinctly not erupting loops, but instead are surge-like jets showing a characteristic inverted-Y spike shape similar to the Eiffel tower. Because this shape is compatible with the Shibata reconnection model, it has implications for the network activity that generates spicules and that may drive coronal heating and solar wind acceleration in quiet regions and coronal holes.

2. Observations and Image Processing

We used full-disk line-center Hα movies from the BBSO synoptic telescope (Denker et al. 1999). The cadence is 1 to 3 minutes, and the spatial resolution is $\approx 2''$ ($= 1''$ pixel^{-1}). We selected the following six days at solar minimum: 1996 August 25, 1996 August 28, 1996 September 7, 1996 October 16, 1997 April 14, and 1997 May 7. On each day there were 5 to 10 hours of observations. Full-disk He II 304 Å images from SOHO/EIT showed that north and south polar coronal holes were present on the limb on each day. We used these He II 304 Å images to identify the arc of limb covered by each coronal hole in the Hα images. After processing the Hα images as described below, we made mpeg movies and identified macrospicule limb events in the polar coronal holes using criteria based on previous studies of macrospicules (e.g., Bohlin et al. 1975). The selection criteria for the macrospicules in our set are: (1) it is located on or near the limb in a polar coronal hole, (2) it is bright above the limb, (3) it extends above the limb to heights greater than 15,000 km, and (4) it is observed from start to end. The fourth criterion is important for correctly classifying a macrospicule's structural type (loop, spike, or unclassifiable), for measuring the lifetime, and for observing the evolution of the entire event.

The original Hα images contain limb darkening and scattered light, hindering the visibility of features near the limb. To bring out faint features near and above the limb, we processed each image as follows. Adopting the method of Georgakilas et al. (1997), in each image we calculated the average intensity on concentric circles from disk center out to 0.2 solar radii above the limb. For example, for the image at 15:46 UT on 1997 May 7, the resulting radial profile of the mean intensity is shown in Figure 2a. As Georgakilas et al. (1997) reported, subtraction of the mean intensity profile from the original image removes the steep intensity gradient near the limb and gives improved visibility to faint features at and above the limb. The two lower panels in Figure 2 demonstrate this improvement in the example image along part of the northern limb. In particular, a macrospicule on the limb, the dark base of the spicule band along the limb, and the chromospheric network inside the

limb are all much more visible in the residual image (Figure 2c) than in the original image (Figure 2b). By viewing movies of the residual images, and by frame-by-frame scrutiny, we identified and studied the macrospicule events that satisfied our four selection criteria.

3. Results

3.1. Dichotomy of Magnetic Structure: Loops and Spikes

From the 6 days of Hα movies, we found 35 macrospicules that were observed from the beginning to the end in the polar coronal holes. These 35 events are listed in Table 1. The histogram of the lifetimes is shown in Figure 3a. The average lifetime is 10.0 ± 3.9 minutes, which is consistent with previous observations (e.g., Bohlin et al. 1975). A large majority of these macrospicules (32/35) could be discerned to have one or the other of two different forms. A large minority (15/35) had the form and evolution of an erupting loop. Most of the rest (17/20) had the form and evolution of a single-column spiked jet shooting up from a broader base. Only a small minority (3/35) did not decidedly display either of these two dominant forms; these were categorized as being of unclassifiable form. The histogram in Figure 3a shows no significant difference in average lifetime among the three categories. That 43% of our macrospicules appear to be erupting loops, we consider to be strong evidence that network-scale erupting magnetic loops are a common occurrence in polar coronal holes. In the following subsections, we present examples of each of the two main structural types of Hα macrospicules.

3.2. Erupting-Loop Macrospicules

One of the erupting-loop macrospicule events is shown in Figure 4. This event appears to be seated slightly on the far side of the limb, so that in the first frame of Figure 4a the top edge of the erupting loop was just beginning to rise into view from behind the limb. A minute later, in the second frame, the loop has risen higher and was seen as an arch standing on the limb. Another minute later, the top of the arch has become nearly too faint to be seen. Thereafter, in the final three frames, only the two legs of the erupting loop remained visible. These become taller and fainter as they continued to move apart.

The fifth frame of Figure 4a is from the same Hα image as in Figure 2c and shows the same macrospicule. This illustrates the importance of observing the entire life of a macrospicule for certifying whether it is an erupting-loop event or a spiked-jet event. From only a single snapshot such as Figure 2c, it would be uncertain whether the two columns

were two spiked-jet macrospicules or the two legs of an erupting-loop macrospicule.

The image sequence in Figure 4a might give the impression that the top of the loop may have been breaking open around the time of the third frame. We think that the loop did not open at this stage, but continued to erupt much higher before being opened by reconnection with the ambient field in the coronal hole. This reconnection should open the erupting loop on the side (as in Figure 1) rather than on the top. During the time covered in Figure 4a, instead of the loop top being opened by reconnection, we think that the top became invisible in these images because of decreasing mass density and content, from expansion of the erupting magnetic loop and from gravitational draining of material from the top of the loop down the legs. This effect is often seen in Hα movies of erupting filaments, and our erupting-loop macrospicules appear to us to be small-scale versions of erupting filaments. Small erupting-filament events of the scale of macrospicules have been observed in quiet regions on the disk in high-resolution Hα movies (Hermans & Martin 1986; Wang et al. 2000).

Figure 4b is a time plot of the measured height and base width of the erupting-loop macrospicule in Figure 4a. This shows that the height and base width increased by about a factor of 3 over the course of the event. Apparently, the feet of the erupting loop migrated away from each over by moving across the solar surface. Similar foot migration is also often seen in large filament eruptions (e.g., Hori 2000).

Another erupting-loop macrospicule event is shown in Figure 5. This event appears to be seated right at the limb. In the first frame of Figure 5a, the macrospicule was seen as a bright arch standing on the limb. In the second frame, 45 seconds later, the loop has erupted farther up and its feet are farther apart. In the final three frames, the loop was much fainter, but could be discerned to continue to expand. In the final frame, the top of the loop was no longer visible and the eastern leg was barely visible. The time plot of the height and base width in Figure 5b shows that the loop became taller by a fact of 1.7 while it became wider by a factor of 2.5.

The two macrospicule events in Figures 4 and 5 are similar in their form and evolution, and they are representative of our erupting-loop macrospicules. The initial and maximum base widths listed in Table 1 show that most of our erupting-loop macrospicules increase in base width as they erupt upward, but the factor of increase is often less than 2. The two erupting-loop macrospicules in Figures 4 and 5 appear to be viewed nearly exactly from the side. The same events viewed more nearly end-on to the loop would show less increase in base width, and this could yield a smaller factor of increase.

3.3. Spiked-Jet Macrospicules

One of the spiked-jet macrospicule events is shown in Figure 6. In the first frame of Figure 6a, the event began as a bright point or mound on the limb. Over the next seven minutes (in frames 2 through 8), the mound grew in height and width and a spiked jet shot up from the top of the mound, so that the macrospicule acquired the inverted-Y shape of the Eiffel tower. In frame 8, the jet was fading. In the final five frames after frame 8, the remnants of the jet and mound were faint and blurred, and therefore the heights and mound base widths of this spiked-jet event plotted in Figure 6b are less certain than in the first eight frames. Both the images (Figure 6a) and the time plot of the height and mound base width (Figure 6b) show that the event continuously grew during the first seven minutes of the event.

The sketch in Figure 6c indicates how the observed form and evolution of this macrospicule fit the Shibata reconnection model for X-ray jets and Hα surges. The advent of the bright point in the first frame of Figure 6a could correspond to the onset of explosive reconnection between the positive-polarity (western) leg of a network-scale closed bipole and the contiguous negative-polarity open field of the southern polar coronal hole. Downward, this reconnection will build new closed loops on the west side of the parent bipole. Upward, the reconnection will produce and release slingshot-like dynamic open field lines that are rooted on the east side of the parent bipole and that drive the jet up from the top and east side of the parent bipole. As the reconnection continues, the new closed loops will become progressively wider and taller, and the new released slingshot field lines will be rooted progressively farther east. As long as the reconnection continues, the jet will continue to be fed and the inverted-Y base of the macrospicule will grow in width and height. When the reconnection stops, the base will stop growing, and the base and jet will fade to invisibility, as in the final six frames of Figure 6a.

Another spiked-jet macrospicule event is shown in Figure 7. It appears that this event may be seated slightly on the far side of the limb. In the first frame of Figure 7a, the bright point may have been the top of a jet-base mound that was rising from behind the limb. Over the next three minutes (frames 2, 3, 4), a jet began to extend up from the top and west side of this base. During the next three minutes (frames 5, 6, 7), the jet became taller, and a low bright arch feature (pointed at by the arrows) appeared and widened to the east of the jet. In frames 5 and 6, the resulting overall form of the macrospicule was reminiscent of an inverted Y. After frame 7, the low arch was no longer definitely visible, and the jet gradually faded out.

The measured base widths plotted in Figure 7b include the low arch in frames 5, 6, and 7. After frame 7, the low arch was too indistinct for its width to be measured, and only the

width of the base of the column of the jet was measured. The measured heights increased in the first six minutes. The heights over next six minutes fluctuated around $\sim 20,000$ km, which suggests that magnetic reconnection would continue to take place intermittently on the base of this event after its height reached the maximum in contrast to Figure 6. Both the images (Figure 7a) and the time plot (Figure 7b) show that from the onset of the event until the low arch and the jet both began to fade, the height and base width of this spiked-jet macrospicule continued to increase.

The sketch in Figure 7c shows how the Shibata reconnection model fits this macrospicule in the same manner as for the macrospicule in Figure 6. The east-west magnetic arrangement in Figure 7c is the reverse of that in Figure 6c. To fit the form and development of the macrospicule in Figure 7a, the reconnection needs to be on the east side of the parent bipole, at the interface between the negative-polarity (east) leg of the parent bipole and the contiguous positive-polarity open field of the northern polar coronal hole. Then the closed loops released downward from the reconnection site could build the low arcade east of the jet, and the slingshot open field lines released upward could drive the jet. The explosive reconnection would start at or before the time of the first frame of Figure 7a. The low arch would start to build as soon as the reconnection started, but would be hidden behind the limb until reaching high enough altitude to become visible above the limb, as in frame 5.

The two spiked-jet macrospicule events in Figures 6 and 7 were similar in their form and evolution. When they were fully developed, they both showed roughly the overall shape of an inverted Y. Up until the macrospicule started to fade, the base of the inverted Y grew in height and width. This behavior is characteristic of all of our spiked-jet macrospicule events. The base width of the spiked-jet macrospicule in Figure 6 grew by a factor of 4, and the base width of the spiked-jet macrospicule in Figure 7 grew by a factor of 2. Most of our spiked-jet macrospicules did show growth in base width, but often not this much (Table 1). Because all of our spiked-jet macrospicules are similar to the examples in Figures 6 and 7, we think that they are all compatible with the Shibata reconnection model, and hence are evidence for explosive reconnection between open and closed magnetic fields low in the magnetic network in coronal holes.

The maximum base widths of the two examples of the spiked-jet macrospicules (Figures 6b and 7b) are noticeably less than the maximum base widths of the two examples of the erupting-loop macrospicules (Figures 4b and 5b): 8000 km and 7900 km versus 15,000 km and 12,200 km (Table 1). As the histogram in Figure 3b shows, this difference is characteristic of our sample. That is, the spiked-jet macrospicules tend to be narrower than the erupting-loop macrospicules: the average maximum base width of our 17 spiked-jet macrospicules is about 7000 km, whereas the average maximum base width of our 15 erupting-loop macrospicules

is about 11,000 km. The velocity histogram of our 35 macrospicules (Figure 3c) indicates two other differences. First, the range of velocities is wider for spiked-jet macrospicules than for the erupting-loop macrospicules. Second, the averaged velocity of the 17 spiked-jet macrospicules (42 ± 19 km s^{-1}) is somewhat faster than that of the 15 erupting-loop macrospicules (32 ± 10 km s^{-1}). [It should be noted that the velocity was derived from the two data points of the time and height from the first and last frames in the rising phase of each event. The velocities shown in Figure 3c consistent with previous studies (Bohlin et al. 1975; Dere et al. 1989; Karovska & Habbal 1994)]. Perhaps these quantitative differences are linked with a basic qualitative difference in the way the two kinds of macrospicule are driven. The spike-jet macrospicules show good evidence of arising via reconnection between network-scale closed magnetic field and open magnetic field of the coronal hole. In contrast, the erupting-loop macrospicules show no evidence for such reconnection; instead, they appear to be an eruption of closed field as in a filament eruption.

4. Discussion

With the initial intent of looking for erupting-loop macrospicules in the magnetic roots of the high-speed polar wind, we processed the images from BBSO full-disk Hα movies to enhance the visibility of features at and near the limb. From a search of the limb in the north and south polar coronal holes in movies of about 40 hours, we found 35 macrospicules that were observed from the beginning to the end with time resolution of 1 – 3 minutes and spatial resolution of roughly $2''$. All but 3 of these macrospicules showed one or the other of two different magnetic forms: 15 were erupting-loop macrospicules and 17 were spiked-jet macrospicules. The form and evolution of an erupting-loop macrospicule are similar to those of a filament eruption, whereas the form and evolution of a spiked-jet macrospicule are similar to those of Hα surges and X-ray jets.

Macrospicules are so named because they have the general appearance of giant spicules. This suggests that spicules are smaller versions of macrospicules, namely, finer-scale eruptions that are driven in the same way. Tanaka (1972, 1974) found that about 30% of Hα spicules observed with subarcsecond resolution on the disk have double-column structure. The tops of our erupting-loop macrospicules fade to invisibility as the loop erupts, so that during much of the event only the two legs of the erupted loop remain visible, giving the macrospicule a double-column structure. The fraction of our macrospicules that are erupting-loop (double-column) macrospicules (43%) is comparable to the fraction of spicules that show double-column structure. This result bolsters the idea that Hα macrospicules are the large-scale extreme of a much more numerous network population of fine-scale Hα eruptions, most of

which are spicules. More specifically, that the erupting-loop fraction of Hα macrospicules is similar to the double-column fraction of Hα spicules lends support to our suggestion that double-column spicules might be erupting-loop events. In addition, that nearly all of those Hα macrospicules that are not erupting-loop macrospicules are spiked-jet macrospicules suggests that most spicules that are not double-column might be finer-scale versions of spiked-jet macrospicules.

Fisk, Schwadron, & Zurbuchen (1999) suggest that the magnetic reconnection between small magnetic loops which emerge within supergranules and open magnetic field provides Poynting flux and mass flux sufficient for the coronal heating and the acceleration of the high-speed solar wind. The magnetic topology of their model is the same as that for the formation of a magnetic switchback from an erupting-loop macrospicule (Figure 1) and the same as that for our spiked-jet macrospicules (Figures 6c and 7c). Moreover, the size of the emerging loops in their model is $\sim$ 10,000 km, which is about the base width of our Hα macrospicules. Therefore, the magnetic structure of our Hα macrospicules in coronal holes supports the reconnection model of Fisk, Schwadron, & Zurbuchen (1999). However, the number of Hα macrospicules obtained from BBSO Hα observations with our selection criteria is too small to generate Poynting flux sufficient for the heating of the corona and the acceleration of the high-speed solar wind. On the other hand, the He II 304 Å images from SOHO/EIT show many more macrospicules extending above 15,000 km in coronal holes than do the BBSO full-disk Hα images, 10 to 100 times more. As a next step, we plan to investigate the birth rate and magnetic structure of EUV macrospicules in coronal holes using SOHO and TRACE EUV data as well as BBSO Hα data.

From modeling of observed properties of the fast solar wind from coronal holes, together with physical reasoning, Axford & McKenzie (1992, 1997) advocate that (1) the corona and solar wind in and from coronal holes are heated and accelerated by high-frequency MHD waves having periods $<\sim$ 1 s, (2) these waves are generated by fine-scale explosive reconnection events (microflares) at polarity reversals low in the magnetic network, and (3) such microflaring activity in the network drives the heating of the corona in quiet regions that are not in coronal holes (Axford & McKenzie 1992, 1997; Axford et al. 1999). Further evidence favoring this scenario for coronal heating in quiet regions and coronal holes was found recently by Falconer et al. (2003). By measuring the luminosity of the corona and comparing it with measurements of the underlying magnetic network observed in the photosphere, they found that the coronal luminosity in quiet regions increases roughly as the square root of the magnetic flux content of the network and roughly in direct proportion to the total length of the perimeter (the coast length) of the many flux clumps composing the network. From this result, they infer that coronal heating in quiet regions is driven mainly by fine-scale magnetic activity in the edges of the network flux clumps. Building on a complementary study by

Moore et al. (1999) of coronal heating in active regions by microflaring in low-lying sheared core fields, Falconer et al. (2003) point out that one plausible possibility is that the inferred activity at the network edges is from embedded stressed closed fields (sheared-core bipoles) that, by exploding, drive reconnection with high-reaching fields rooted against these bipoles. Falconer et al. (2003) estimate that such exploding bipoles could yield enough power for the corona, in the form of MHD waves and energetic particles, provided that the bipoles have diameters of $\sim$ 1000 km, field strengths of a few hundred Gauss, lifetimes of $\sim$ 5 minutes, and $\sim$ 30 are present at any time in the edges of the magnetic network around each supergranule cell. The magnetic configuration proposed by Falconer et al. (2003) for these reconnection events is basically the same as in the Shibata reconnection model for surges and X-ray jets, and hence is appropriate for producing spicules in the same way as for our spiked-jet macrospicules. Thus, because about half of our macrospicules are spiked-jet macrospicules and appear to fit the Shibata reconnection model, we have found evidence favoring the possibility that a comparably large fraction of spicules, the single-column spicules, are driven by similar reconnection, and hence that the network may be peppered by fine-scale reconnection events of the type needed for coronal heating as advocated by Axford & McKenzie (1992, 1997), Moore et al. (1999), and Falconer et al. (2003). The same evidence and reasoning encourage the prediction of Falconer et al. (2003) that the vector magnetograph on the forthcoming Japan/US/UK Solar-B mission (to be launched in 2006) will detect at the base of most spicules, rooted in the edges of the network flux clumps, inclusions of opposite-polarity flux that are $<\sim$ 1000 km in diameter and have field strengths $>\sim$ 100 G.

As was noted in the Introduction, from observation of network-scale magnetic switchbacks in the polar wind (Yamauchi et al. 2003), we expected that the eruption of network-scale magnetic loops should be a common occurrence in polar coronal holes. This expectation has been substantiated by our finding that 43% of our macrospicules were erupting-loop macrospicules. The erupting magnetic loop in these macrospicules could become a magnetic switchback via reconnection with the open magnetic field of the polar coronal hole, as sketched in Figure 1.

From the observed structure of our macrospicules, we infer that, before eruption onset, the basic magnetic setup for an erupting-loop macrospicule is broadly the same as that for a spiked-jet macrospicule: a closed bipole embedded in the feet of the open magnetic field of the coronal hole. One end of the closed bipole must be rooted in a region of polarity opposite to that of the dominant-polarity open field, and there should be a magnetic null at the interface between the bipole and the open field, located on or above the included-polarity side of the bipole, as in the sketches in Figures 6c and 7c. In the Shibata reconnection model for spiked-jet macrospicules, the event starts when explosive reconnection starts at the null. This reconnection could be driven, as proposed by Falconer et al. (2003), by a confined

explosion of sheared field in the core of the parent bipole. In erupting-loop macrospicules, it appears that the erupting loop is an ejective eruption of sheared core field from the parent bipole, as in a filament eruption during the initiation of a coronal mass ejection (e.g., Moore et al. 2001). It is not clear to us why the eruption of the parent bipole in an erupting-loop macrospicule does not appear to drive reconnection at the external null, as in a spiked-jet macrospicule. However, the difference in the observed structure of erupting-loop macrospicules from that in spiked-jet macrospicules suggests that the conditions at the external null are different in some essential way in the erupting-loop events so that the external reconnection does not happen or is much slower than in spiked-jet events, at least until the loop erupts high into the coronal hole.

This work was supported by NASA's Office of Space Science through its Solar and Heliospheric Physics Supporting Research and Technology Program and its Sun-Earth Connection Guest Investigator Program. The work was performed while Y. Yamauchi held a National Research Council NASA/MSFC Resident Research Associateship. We are grateful to the staff at BBSO for their support in obtaining the Hα data.

REFERENCES

Axford, W. I., & McKenzie, J. F. 1992, in Solar Wind Seven, ed. E. Marsch E. & R. Schween, (Oxford: Pergamon Press), 1

Axford, W. I., & McKenzie, J. F. 1997, in Cosmic Winds and the Heliosphere, ed. J. R. Jokipii, C. P. Sonett, & M. S. Giampapa (Tucson: University of Arizona Press), 31.

Axford, W. I., McKenzie, J. F., Sukhorudova, G. V., Banaszkiewicz, M., Czechowski, A., & Ratkiewicz, R. 1999, Space Sci. Rev., 87, 25

Balogh, A., Forsyth, R. J., Lucek, E. A., Horbury, T. S., & Smith, E. J. 1999, Geophys. Res. Lett., 26, 631

Beckers, J. M. 1977, in Illustrated Glossary for Solar and Solar-Terrestrial Physics, ed. A. Bruzek & C. J. Durrant (Dordrecht: Reidel), 21

Bohlin, J. D., Vogel, S. N., Purcell, J. D., Sheeley, N. R., Tousey, R., & Van Hoosier, M. E. 1975, ApJ, 197, L133

Bunmba, V., Klvaňa, M., & Sýkora, J. 1994, ed. V. Rušin, P. Heinzel, & J.-C. Vial, Proc. IAU Colloq. 144, Solar Coronal Structures (Bratislava: VEDA Publ. Comp.), 47

DeForest, C. E., Hoeksema, J. T., Gurman, J. B., Thompson, B. J., Plunkett, S. P., Howard, R., Harrison, R. C., & Hasslerz, D. M. 1997, Sol. Phys., 175, 393

Denker, C., Johannesson, A., Marquette, W. H., Goode, P. R., Wang, H., & Zirin, H. 1999, Sol. Phys., 184, 87

Dere, K. P., Bartoe, J.-D. F., Brueckner, G. E., Cook, J. W., Socker, D. G., & Ewing, J. W. 1989, Sol. Phys., 119, 55

Dowdy, J. F., Jr., Rabin, D., & Moore, R. L. 1986, Sol. Phys., 105, 35

Falconer, D. A., Moore, R. L., Porter, J. G., & Hathaway, D. H. 1998, AJ, 501, 386

Falconer, D. A., Moore, R. L., Porter, J. G., & Hathaway, D. H. 2003, AJ, in press

Fisk, L. A., Schwadron, N. A., & Zurbuchen, T. H. 1999, J. Geophys. Res., 104, 19,765

Forsyth, R. J., Balogh, A., Horbury, T. S., Erdoes, G., Smith, E. J., & Burton, M. E. 1996, A&A, 316, 287

Georgakilas, A. A., Dara, H. C., Zachariadis, Th. G., Alissandrakis, C., & Koutchmy, S. 1997, Sol. Phys., 172, 133

Habbal, S. R., & Gonzales, R. D. 1991, AJ, 376, L25

Hermans, L. M., & Martin, S. F. 1986, in Coronal and Prominence Plasmas, ed. A. I. Poland (NASA CP-2442), 369

Hori, K. 2000, AJ, 543, 1011

Karovska, M., & Habbal, S. R. 1994, ApJ, 431, L59

LaBonte, B. J. 1979, Sol. Phys., 61, 283

Lin, Y., 1994, ed. V. Rušin, P. Heinzel, & J.-C. Vial, Proc. IAU Colloq. 144, Solar Coronal Structures (Bratislava: VEDA Publ. Comp.), 41

Loucif, M. L. 1994, A&A, 281, 95

Moore, R. L., Tang, F., Bohlin, J. D., & Golub, L. 1977, AJ, 218, 286

Moore, R. L., Falconer, D. A., Porter, J. G., & Suess, S. T. 1999, AJ, 526, 505

Moore, R. L., Sterling, A. C., Hudson, H. S., & Lemen, J. R. 2001, AJ, 552, 833

Shibata, K., 1982, Sol. Phys., 81, 9

Shibata K., Ishido, Y., Acton, L. W., Strong, K. T., Hirayama, T., Uchida, Y., McAllister, A. H., Matsumoto, R., Tsuneta, S., Shimizu, T., Hara, H., Sakurai, T., Ichimoto, K., Nishino, Y., & Ogawara, Y. 1992, PASJ, 44, L173

Shibata, K., 2001, in Encyclopedia of Astronomy and Astrophysics, ed. P. Murdin, (Bristol: Institute of Physics Publishing), 3258

Tanaka, K., 1972, Report of Big Bear Solar Observatory, No.125

Tanaka, K. 1974, in Chromospheric Fine Structure, ed. R. G. Athay (Dordrecht: Reidel), 239

Tandberg-Hanssen, E. 1977, in Illustrated Glossary for Solar and Solar-Terrestrial Physics, ed. A. Bruzek & C. J. Durrant (Dordrecht: Reidel), 97

Wang, H. 1998, AJ, 509, 461

Wang, J., Li, W., Denker, C., Lee, C., Wang, H., Goode, P. R., McAllister, A., & Martin, S. F. 2000, AJ, 530, 1071

Withbroe, G.L., Jaffe, D.T., Foukal, P. V., Huber, M. C. E., Noyes, R. W., Reeves, E. M., Schmahl, E. J., Timothy, J. G., & Vernazza, J. E. 1976, AJ, 203, 528

Yamauchi, Y., Suess, S. T., & Sakurai, T. 2002, Geophys. Res. Lett., 29, 10.1029/2001GL013820

Yamauchi, Y., Suess, S. T., Steinberg, J. T., & Sakurai, T. 2003, J. Geophys. Res., submitted

Yokoyama, T., & Shibata, S. 1995, Nature, 375, 42

Yokoyama, T., & Shibata, S. 1996, PASJ, 48, 353

This preprint was prepared with the AAS LaTeX macros v5.0.

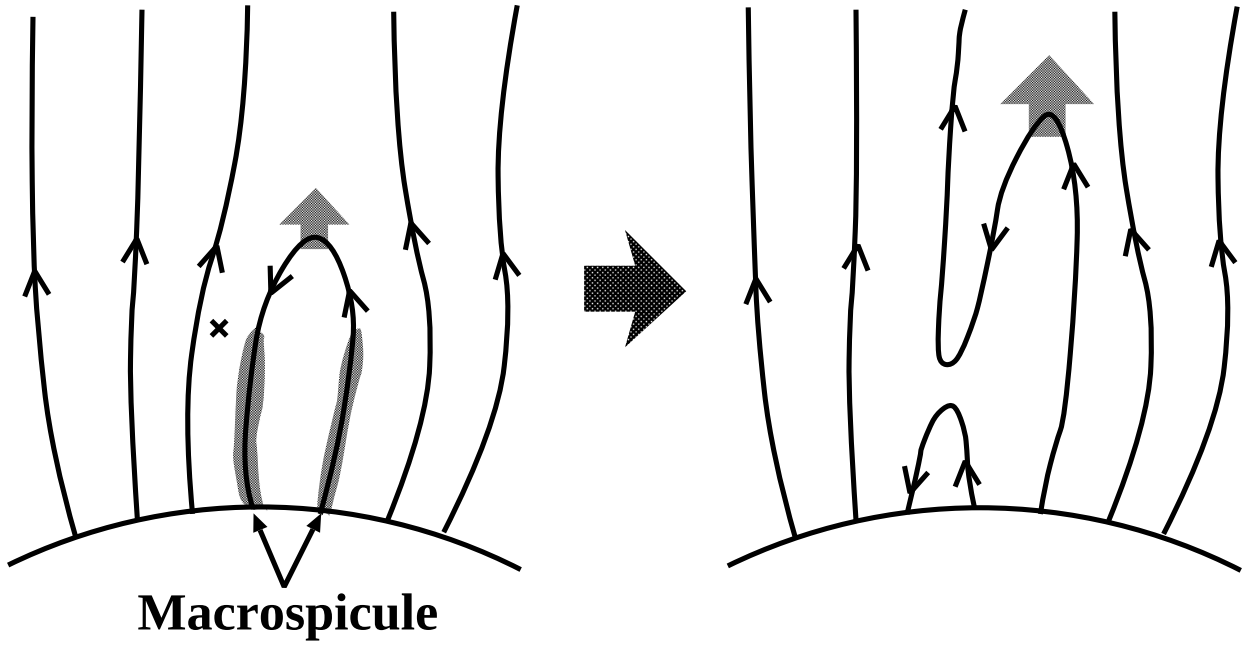

Fig. 1.— Schematic of an erupting-loop macrospicule in a coronal hole and its conversion to a magnetic switchback via reconnection with the unipolar open field of the coronal hole.

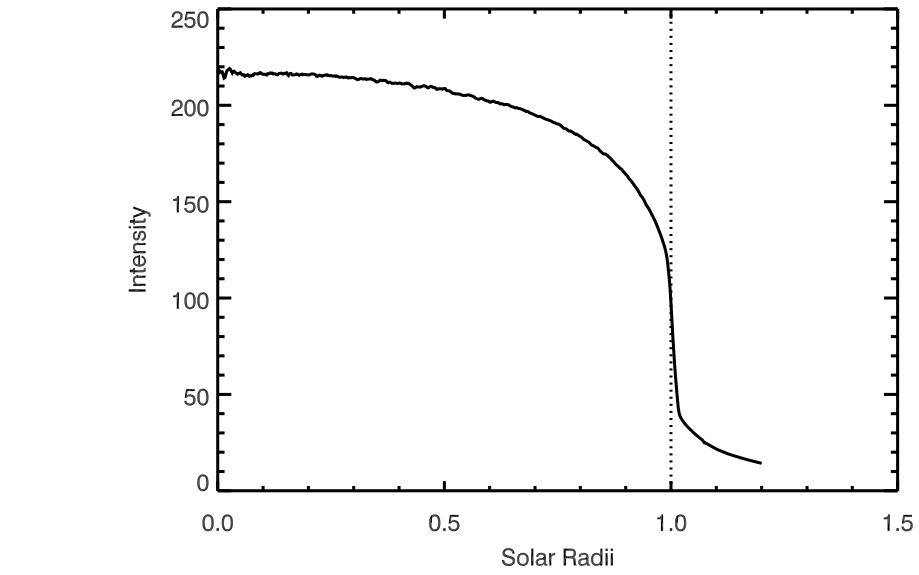

(a)

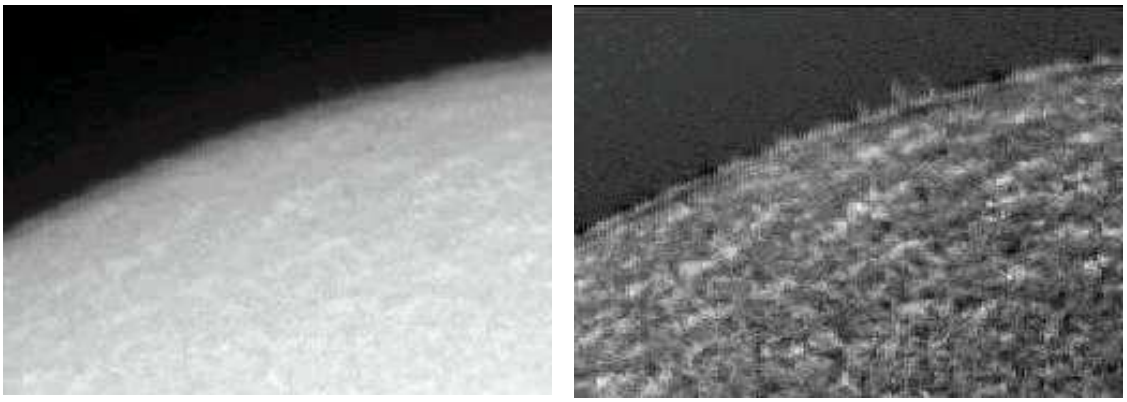

(b) **(c)**

Fig. 2.— Illustration of our image processing of the BBSO full-disk Hα images for enhancing the visibility of features at and near the limb. The example image used here was taken at 15:46 UT on 1997 May 7. Panel (a) shows the average radial profile of the brightness of the image from disk center to 1.2 solar radii, crossing the limb (dotted line) at the solar radius. At distances of more than a few hundredths of a solar radius beyond the limb, most of the brightness is from scattered light. Panel (b) shows a part of the original image, in a field of view covering the eastern part of the north polar limb. Panel (c) shows the improved visibility of chromospheric structure in the processed image, after subtraction of the brightness profile of Panel (a) from the original image.

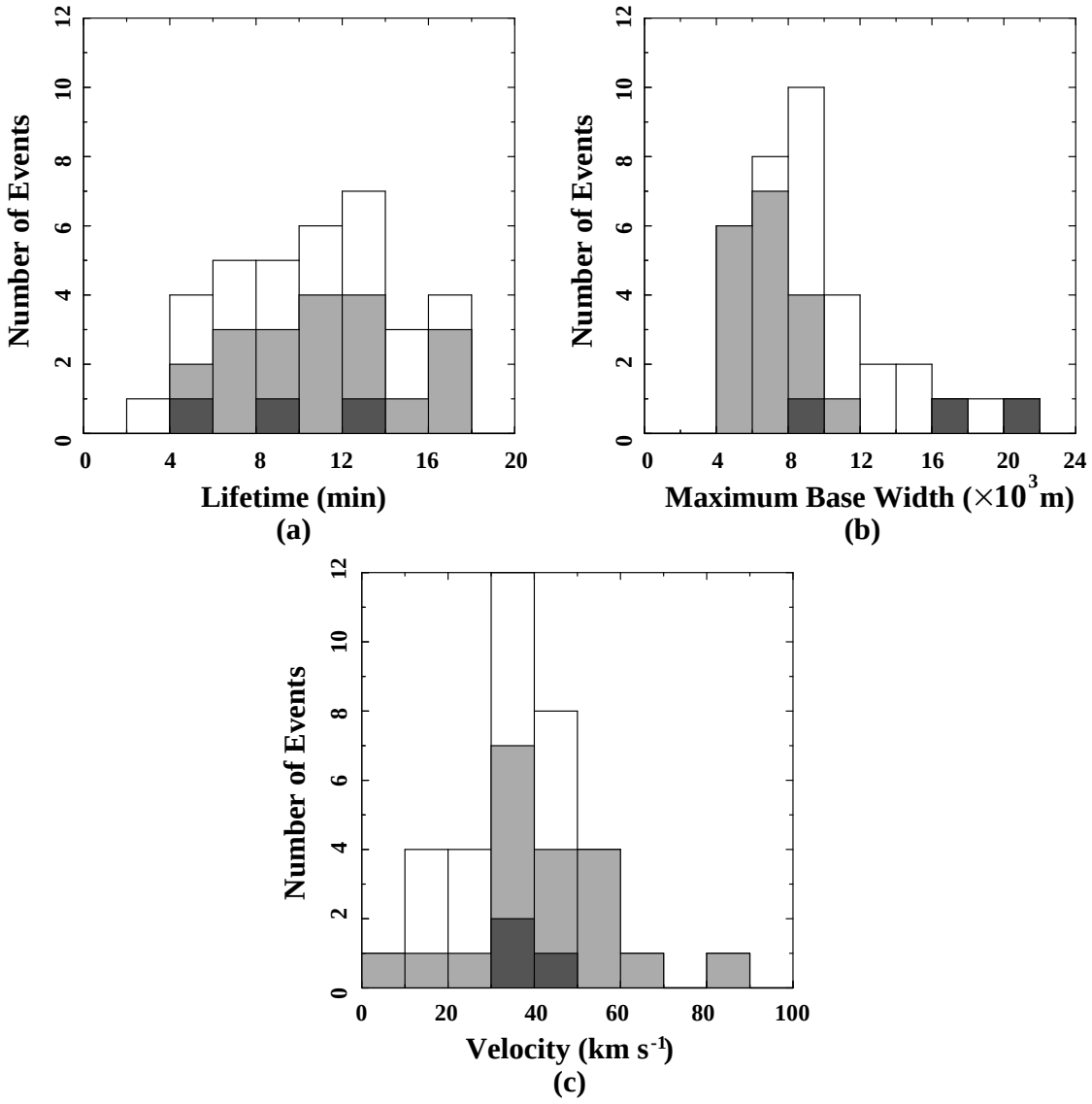

Fig. 3.— Histograms of (a) the lifetimes, (b) the maximum base widths, and (c) the velocity of our 35 Hα macrospicules. The unshaded part is for the 15 erupting-loop macrospicules; the light-gray part is for the 17 spiked-jet macrospicules; and the dark-gray part is for the 3 macrospicules of unclassifiable form.

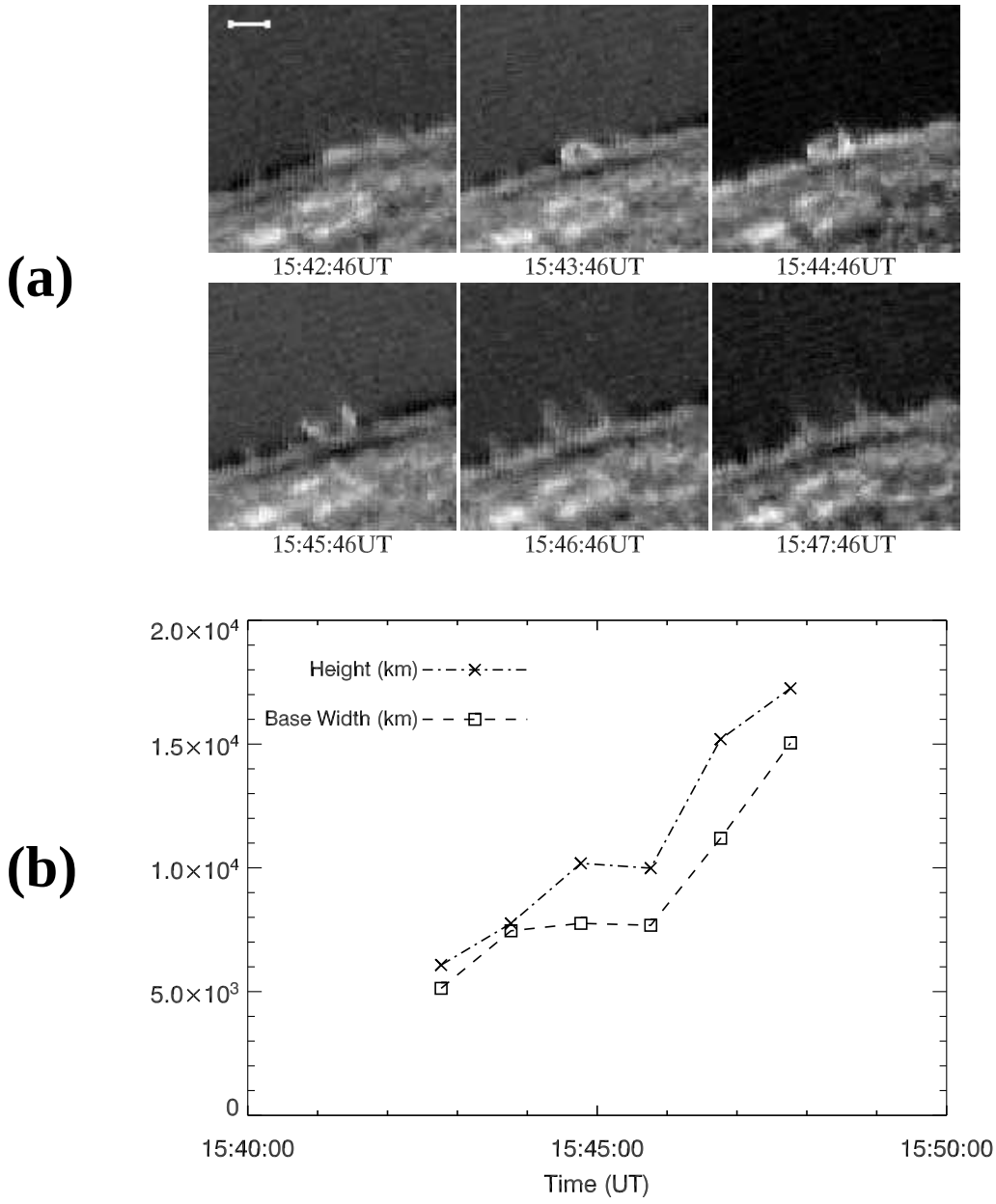

Fig. 4.— The erupting-loop macrospicule observed in the northern polar coronal hole at 15:42-15:47 UT on 1997 May 7. (a) Evolution of the event in the Hα images. The scale bar in the first frame indicates 10,000 km. (b) Evolution of the loop's height and base width. The base width is measured between the outside edges of the two feet.

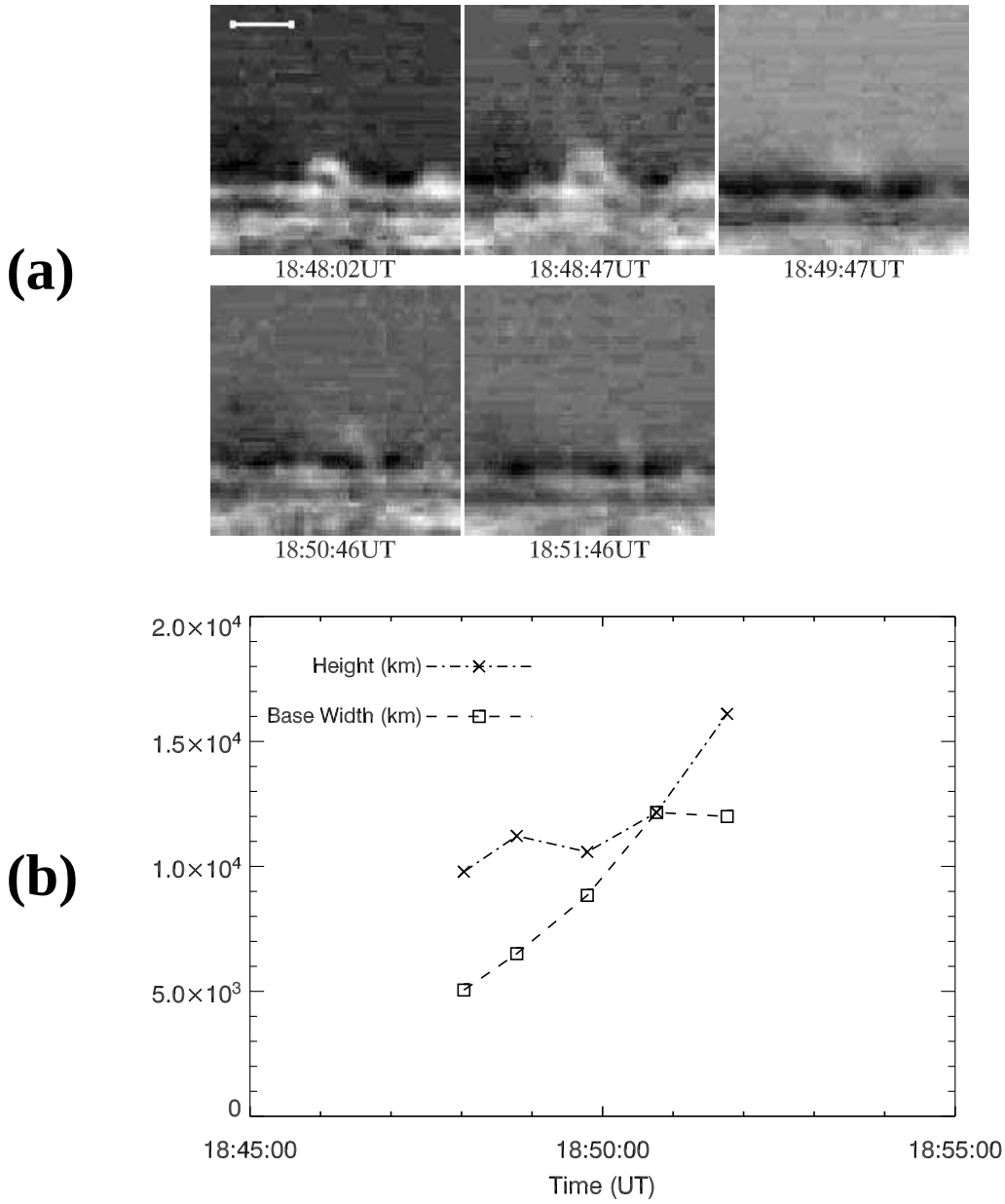

Fig. 5.— The erupting-loop macrospicule observed in the northern polar coronal hole at 18:48-18:51 UT on 1997 May 7. (a) Evolution of the event in the Hα images. The scale bar in the first frame indicates 10,000 km. (b) Evolution of the height and base width of the loop.

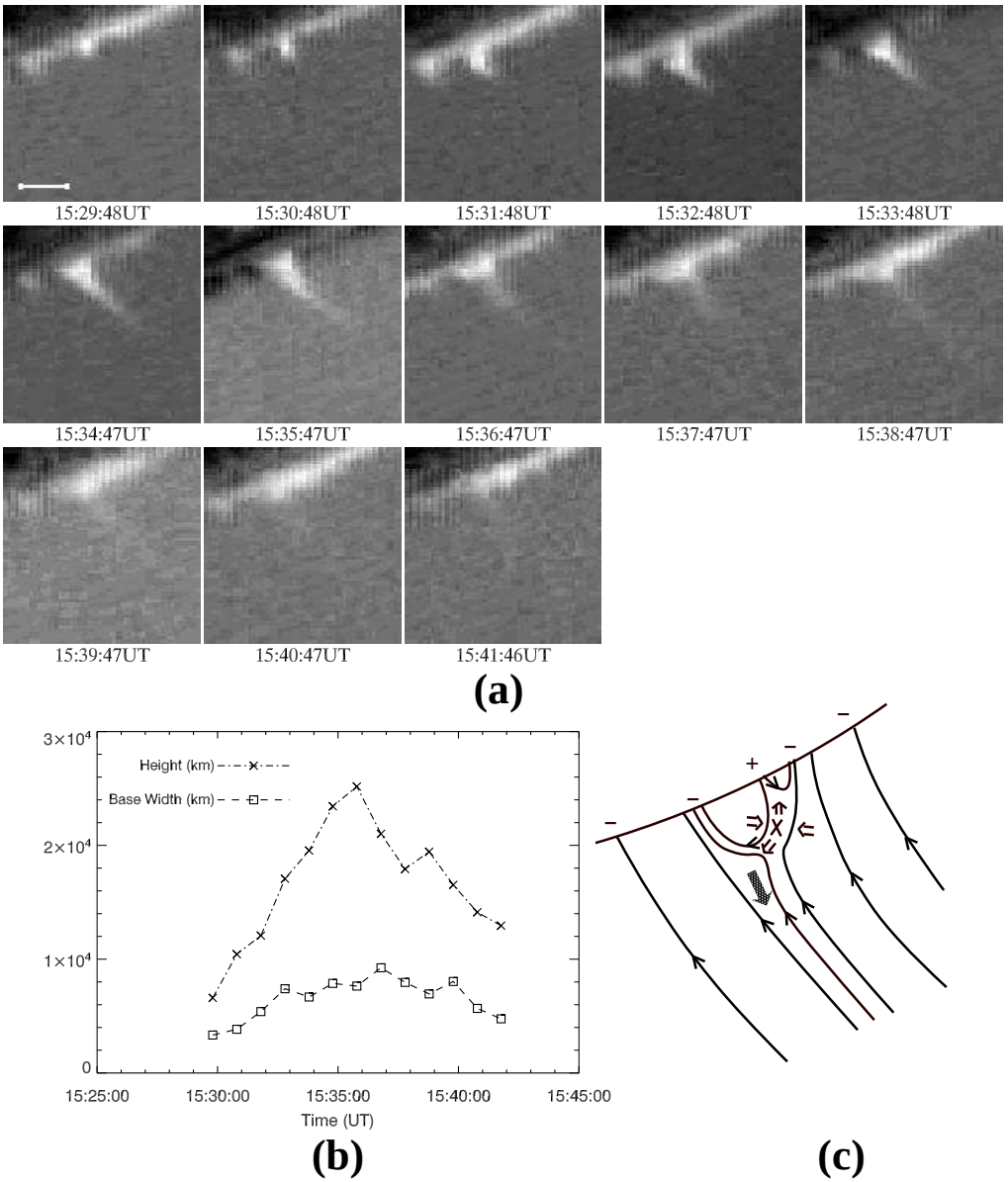

Fig. 6.— The spiked-jet macrospicule observed in the southern polar coronal hole at 15:29-15:41 UT on 1997 May 7. (a) Evolution of the event in the Hα images. The scale bar in the first frame indicates 10,000 km. (b) Evolution of the height and base width. (c) Sketch of the Shibata-style reconnecting magnetic field configuration that fits the observed form and evolution of this event.

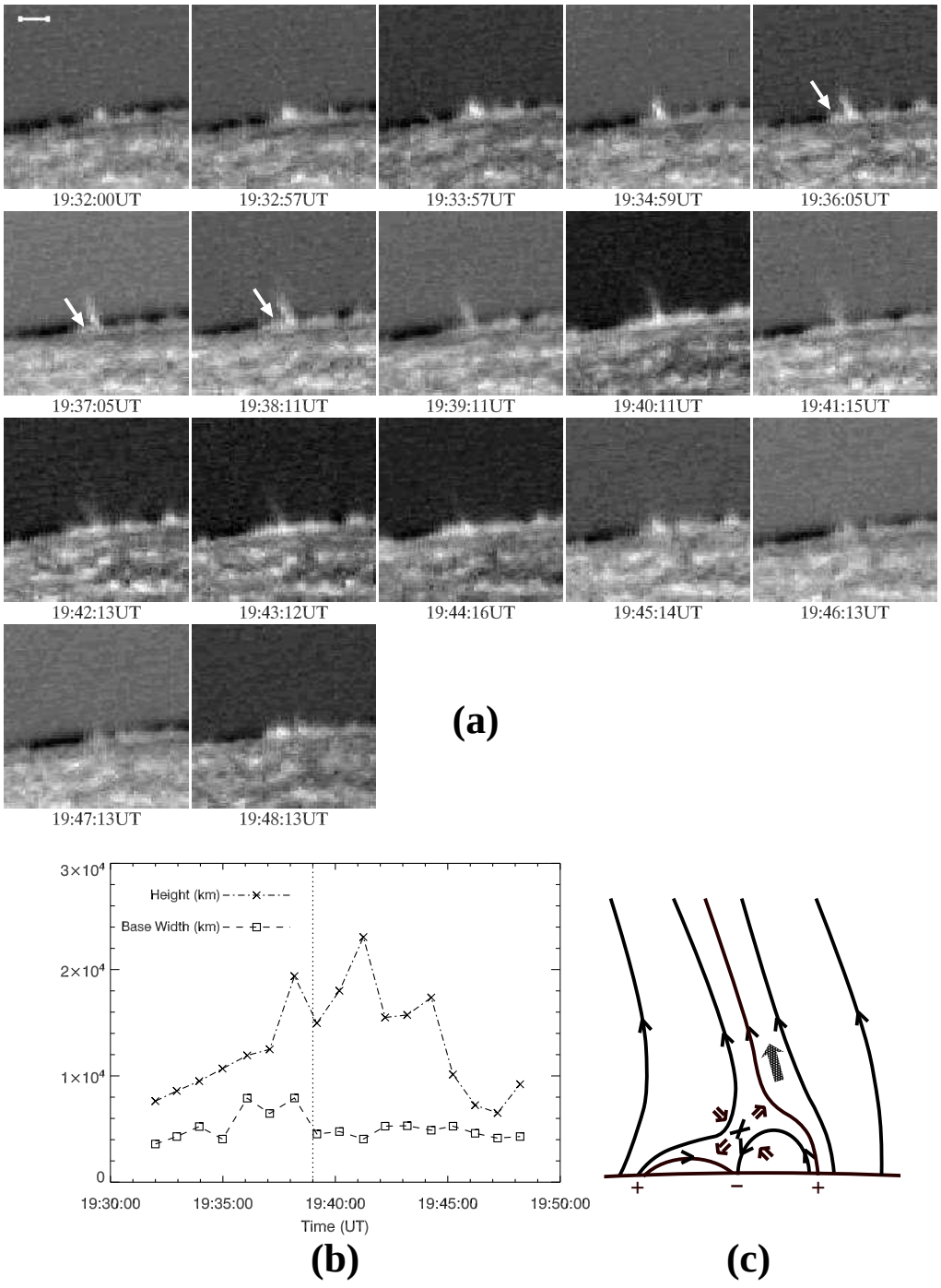

Fig. 7.— The spiked-jet macrospicule observed in the northern polar coronal hole at 19:32-1948 UT on 1996 August 28. (a) Evolution of the event in the Hα images. The scale bar in the first frame indicates 10,000 km. The arrows point to the growing part of the base that corresponds to the new magnetic arch being formed by the reconnection sketched in (c). (b) Evolution of the height and base width. Before 19:39 UT (the time marked by the dashed line), the measured width includes the arch feature east of the jet; after 19:39 UT, this feature has faded out and the measured width includes only the bright base of the jet. (c) Sketch of the Shibata-style reconnecting magnetic field configuration that fits the observed form and evolution of this event.

Table 1: Macrospicule limb events in polar coronal holes

Date	Location	Type	Start Time (UT)	Duration (min)	Maximum Height (10^3 km)	Velocity (km s^{-1})	Initial Base Width (10^3 km)	Maximum Base Width (10^3 km)
1996 Aug 25	59N90W	Loop	14:57	12	22.6	34.5	6.9	18.3
1996 Aug 25	74N90E	Loop	16:43	5	20.2	22.0	10.7	11.4
1996 Aug 25	71N90E	Spike	22:42	8	20.1	36.0	2.6	7.9
1996 Aug 25	87N90W	Unclassifiable	22:46	9	18.1	35.0	12.6	20.1
1996 Aug 25	85S90E	Spike	22:54	4	15.0	15.5	5.5	7.2
1996 Aug 25	87S90E	Spike	24:03	11	19.0	66.8	5.0	5.9
1996 Aug 28	88N90E	Spike	16:27	8	17.9	41.2	2.0	5.3
1996 Aug 28	73S90W	Unclassifiable	17:05	12	23.5	33.5	6.4	16.3
1996 Aug 28	87S90E	Spike	17:22	14	19.2	32.3	4.3	8.5
1996 Aug 28	83N90E	Spike	19:32	16	23.0	31.7	3.6	7.9
1996 Aug 28	87S90W	Loop	20:04	8	18.8	38.3	8.9	14.9
1996 Aug 28	81N90W	Loop	20:20	9	18.1	19.5	5.5	9.3
1996 Aug 28	72S90W	Spike	20:58	10	21.5	54.2	4.0	5.0
1996 Sep 7	78N90E	Loop	17:03	17	24.5	23.0	7.9	9.3
1996 Oct 16	70N90E	Loop	18:12	12	17.0	44.0	6.5	8.1
1996 Oct 16	73N90E	Spike	21:06	12	15.4	9.2	4.2	5.3
1997 Apr 14	78N90E	Loop	17:31	15	16.6	43.6	4.7	8.9
1997 Apr 14	79S90W	Spike	17:38	11	23.1	44.4	5.0	8.1
1997 Apr 14	90S0E	Loop	18:41	14	26.9	46.8	4.7	9.5
1997 Apr 14	89N90W	Loop	18:48	3	16.1	28.2	5.1	12.2
1997 Apr 14	79S90E	Spike	19:44	6	22.8	46.0	6.1	6.1
1997 Apr 14	71S90E	Spike	20:10	6	17.9	34.8	3.7	6.2
1997 Apr 14	90S0E	Spike	20:20	6	32.0	87.8	3.6	5.7
1997 Apr 14	64S90E	Spike	20:30	17	50.7	51.6	3.4	6.8
1997 May 7	69S90W	Spike	15:29	12	25.2	51.7	3.3	8.0
1997 May 7	74N90E	Loop	15:42	5	17.2	37.3	5.1	15.0
1997 May 7	74N90E	Loop	16:40	12	21.9	30.5	3.7	10.3
1997 May 7	69S90W	Spike	16:41	13	17.7	28.7	5.7	10.1
1997 May 7	83N90W	Spike	16:43	10	18.5	57.2	3.0	5.3
1997 May 7	69N90E	Loop	17:03	6	17.7	38.4	4.4	6.0
1997 May 7	64S90W	Loop	17:04	10	19.8	17.1	4.9	11.1
1997 May 7	73N90E	Loop	17:06	10	20.8	42.6	13.0	13.0
1996 May 7	70S90W	Unclassifiable	17:08	5	19.2	47.4	4.0	8.3
1996 May 7	75N90E	Spike	17:21	16	17.7	31.0	4.0	7.2
1997 May 7	89N90W	Loop	18:57	7	15.8	19.3	5.0	9.5